The Journal of Engineering

The 9th International Conference on Power Electronics, Machines and Drives (PEMD 2018)

IET Journals
The Institution of Engineering and Technology

Finite element analysis of a modular brushless wound rotor synchronous machine

eISSN 2051-3305
Received on 25th June 2018
Accepted on 30th July 2018
E-First on 4th June 2019
doi: 10.1049/joe.2018.8206
www.ietdl.org

Huong Thao Le Luong[1,2] ✉, Carole Hénaux[2], Frederuc Messine[2], Guilherme Bueno-Mariani[1], Nicolas Voyer[1], Stefan Mollov[1]

[1]*Power Electronic Systems Department, Mitsubishi Electric R&D Centre Europe (MERCE), Rennes, France*
[2]*GREM3, Laboratoire Plasma et Conversion d'Energie (LAPLACE), Toulouse, France*
✉ *E-mail: hleluong@laplace.univ-tlse.fr*

Abstract: This study presents a comparative study of different modular brushless wound rotor synchronous machines (MB-WRSM) using non-overlapping fractional slot double-layer concentrated windings. The goal of the study is to highlight the structure which offers the best fault-tolerance capability and the highest output performance. The fundamental winding factor is calculated by using the method based on voltage phasors as a significant criterion to select the preferred numbers of phases, stator slots, and poles. With the limited number of poles for a small machine (3.67 kW/7000 rpm), 15 different machines for different phase/slot/pole combinations are analysed using two- dimensional (2D) finite element method and compared according to three criteria: torque density, torque ripple, and machine efficiency. The seven-phase/seven-slot/six-pole machine is chosen with the best compromise of high torque density, small torque ripple (3.89%), and high nominal efficiency (95%). This machine is then compared with a reference design surface-mounted permanent magnet synchronous machine (SM-PMSM). The simulation results are discussed and demonstrate that the MB-WRSM presents interesting performance features, such as extended field weakening range, with overall performance closely matching that of an equivalent SM-PMSM.

1 Introduction

Nowadays, compressors in heating, ventilation and air conditioning (HVAC) use frequently permanent magnet synchronous machine (PMSM) because of its high torque density and efficiency. However, magnet materials are more and more expensive. Therefore, other types of machines with lower cost and good performance are considered to replace PMSM [1, 2]. In particular, modular brushless wound rotor synchronous machines (MB-WRSM) have several advantages such as low cost, a wide field weakening region at high speed, and theoretical torque density close to that of a PMSM [3, 4].

This paper presents a comparative study between different MB-WRSMs. The power supply of this modular structure is chosen in a way that each stator plot is or not supplied by an independent converter. In this case, the motor does not necessarily operate with a stator rotating field and the power supply strategy can be optimised to improve the efficiency in respect of the magnetic field generated by field winding. Besides, the structure exhibits inherent redundancy.

The selection of phase, slot, and pole combination, as well as the winding configuration, is a critical issue to achieve high torque density and efficiency. The preferred number of phases, slots, and poles is usually identified based on the fundamental winding factor, cogging torque, and rotor losses. This paper considers the fundamental winding factor as the main factor of choice for the winding configuration. The choice is made for the fundamental winding factor that provides the highest value in order to maximise the average torque.

With the most suitable winding configurations, 2D finite element method (FEM) was used to determine the performance of the WRSM machine. The numerical simulation permits to accurately evaluate the average torque, the cogging torque, and the power factor. The main goal of this paper is to design high-performance multiphase WRSMs with non-overlapping fractional-slot concentrated winding that can be used to replace PMSM in HVAC applications [5–7].

In the second part of the paper, the calculation of the winding factor and the choice of the winding configurations to be tested will be explained. Moreover, the design of the machine on the FEM software and the efficiency calculation will be also explained. The third part addresses the analysis of the different solutions and the choice of the preferred machine. The comparison with an SM-PMSM is made in the fourth part. Finally, a conclusion is made about the method and the results obtained.

2 Design procedure

2.1 Winding factor calculation

Electrical machines with non-overlapping concentrated winding have been recently investigated for many applications due to the several advantages such as high fault-tolerance capability, easier manufacturing, and significant reduction of copper losses in the end winding [8–11]. The selection of phase/slot/pole combinations is a critical issue to maximise the fundamental winding factor and thus the torque. The various combinations of slots and poles which allow the realisation of a balanced winding can be determined by (1) in the case of the multiphase machine:

$$\frac{Q}{|\mathrm{GCD}(Q, 2_p)|} = km \tag{1}$$

where Q is the number of slots, p is the number of pole pairs, m is the number of phases, k is a positive integer, and GCD is the greatest common divider.

For a specific slot/pole combination and number of phases, there are many possibilities to arrange the coils of each phase in the slots to form the winding layout. The procedure for laying out multiphase concentrated winding configurations in an optimal way was presented in [9], in which the winding factor is investigated by using the method based on the voltage phasors. This method is based on the decomposition of the number of slots per pole and per phase q in its most simplified fraction. For values below unity, q must be reduced to a fraction of two non-divisible integers (b and c) as

$$q = b/c \tag{2}$$

One-zero sequences are established due to (2). The sequence is a list of c numbers that characterise the winding distribution. The number of '1' in the sequence is equal to b and the number of '0' is equal to $c-b$. Considering that many one-zero sequences are created from the specific number of slots per pole and per phase when changing the position of the number '1' and the number '0', many winding layouts can be created and therefore we obtain many different values of a fundamental winding factor. It is thus necessary to select the optimum one-zero sequence with the highest fundamental winding factor. In general, the structure of the whole winding can be fully determined in five steps [11]:

- In the first step, the one-zero sequence is created based on the number of slots per pole and per phase.
- The sequence is repeated Q/b times.
- The usual phase sequence (e.g. AC′BA ′CB' for a three-phase machine) is assigned to the aforementioned number sequence.
- The conductors associated with the number '1' are selected to form the first layer of the winding.
- The second layer of the winding is obtained by shifting the first layer on the other side of the tooth and reversing the phase direction.
- The final winding layout of one phase is created. This layout is numbered by slots, from 1 to Q. For each slot, which contains a conductor of the one phase, the number of the slot with the sign of the phase is written in S.

In the last step, a vector $\boldsymbol{S}$ is produced in order to calculate the fundamental winding factor for non-overlapping fractional-slot double-layer concentrated winding. This vector is used to obtain the voltage phasor $\vec{E}_1$ of a coil side i from phase A for the main harmonic rank, which is defined by (3):

$$\vec{E}_l = \text{sign}(\boldsymbol{S}(i)\text{e}^{j((\pi\times 2p)/(Q))|S(i)|} \tag{3}$$

The fundamental winding factor is represented for non-overlapping fractional-slot double-layer concentrated winding as

$$k_{w1} = \frac{m}{2Q}\left|\sum_{i=1}^{2Q/m}\vec{E}_l\right| \tag{4}$$

where i is one element of S.

Table 1 shows the fundamental winding factors for different phase/slot/pole combinations with the maximum number of poles limited to 10. This limitation of poles is due to a manufacturing issue for small machines.

The fundamental winding factors for the case of a number of phases equal to the number of stator slots is presented in Table 2. The winding configurations with fundamental winding factor >0.9 are selected for the corresponding WRSMs to be analysed by FEM.

2.2 Electromagnetic analysis

In FEM tool, the instantaneous electromagnetic torque is calculated by the local virtual work method (VWM). This method calculates the global and local forces. According to the principle of VWM, the energy balance of an electromechanical system is calculated. The force is thus produced and applied to nodes in the finite mesh elements [12]. For modelling the machine, five principal steps are shown in Fig. 1.

Based on FEM, salient-pole WRSMs are modelled for appropriate phase/slot/pole combinations presented in Fig. 2.

In this kind of machine shown in Fig. 3, each tooth without tips is fabricated separately. The winding is wound automatically around the tooth. After the coils are wound, the stator is bent and press fitted into a frame. Its advantages are ease of assembly, easier to replace faulted components, and high copper area. Besides, each phase can be separately supplied with a drive module so that it operates independently. It allows the system to continue its operation even if a failure occurs.

In order to get the highest average torque with the smallest excitation and armature currents, it is necessary to predetermine the initial position of the rotor as well as the position of the rotating magnetic field in the air gap [13]. One simulation is then carried out at rated speed. The rotor winding is fed with DC and the stator windings are fed with imposed constant currents, e.g. $(I_s, -I_s/2, -I_s/2)$ for a three-phase stator winding. The static torque vs mechanical rotor position curve for a WRSM machine is shown in Fig. 4.

2.3 Efficiency calculation

The efficiency constitutes the main criterion of selection. As a consequence, it is important to well evaluate the losses. Typically, there are three principal types of losses in the machine: (i) the iron losses; (ii) the copper losses; and (iii) the mechanical losses.

2.3.1 Iron losses: The iron losses are located in the magnetic parts of the machine, for example, in the yoke, the teeth etc… They can be distinguished into three components: hysteresis loss, eddy current losses, and excess losses [14] as

$$p_{\text{iron}} = p_{\text{hys}} + p_{\text{edd}} + p_{\text{ex}} \tag{5}$$

where p_{iron} is the iron losses, p_{hys} is the hysteresis losses, p_{edd} is the eddy current losses, and p_{ex} is the excess losses.

These losses can be calculated by the finite element analysis. Iron losses (in watts per cubic meter) are calculated [12] as

$$p_{\text{iron}} = K_{\text{h}}B_{\text{max}}^2 f + K_{\text{c}}(B_{\text{max}}f)^2 + K_{\text{e}}(B_{\text{max}}f)^{1.5} \tag{6}$$

where K_{h} is the hysteresis coefficient, K_{c} is the classical eddy coefficient, K_{e} is the excess or anomalous eddy current coefficient due to magnetic domains, f is the frequency, and B_{max} is the maximum amplitude of the flux density.

2.3.2 Copper losses: The copper losses in electric machines are the losses created by the current in the winding of the machine. In order to estimate the value of the resistance of the coil, it is necessary to evaluate the length of the coil (l_{coil}) as

$$l_{\text{coil}} = 2L_{\text{m}} + l_{\text{end}} \tag{7}$$

where L_{m} is the length of the machine and l_{end} is the length of the end winding.

The average length of the end winding of non-overlapping concentrated winding is

$$l_{\text{end}} = \frac{1}{2}\left(2W_{\text{tooth}} + \pi\frac{\tau_s - w_{\text{tooth}}}{2}\right) \tag{8}$$

where w_{tooth} is the width of stator tooth and τ_{s} is the length of slot pitch.

With the length of one conductor and the area of one conductor, the resistance of one slot of the stator (R_{slot}) is described by

$$R_{\text{slot}} = \rho n_{\text{s}}\frac{l_{\text{coil}}}{A_{\text{coil}}} \tag{9}$$

where A_{coil} is the coil area, ρ is the conductivity coefficient, and n_{s} is the number of conductor per slot.

Considering the resistivity of copper as a function of the temperature, ρ is calculated as

$$\rho = \rho_o(1 + \alpha(T - 20)) \tag{10}$$

where ρ_o is the conductivity coefficient at 20°C, T is the working temperature, and α is the temperature coefficient of resistance for the conductor material.

The resistance of one phase R_{ph} is

Table 2 Multiphase windings with $Q = m$

$Q\|2_p$	2	4	6	8	10
3	0.866	0.866	—	0.866	0.866
4	—	—	—	—	—
5	0.588	0.951	0.951	0.809	—
6	—	—	—	—	—
7	0.434	0.782	0.975	0.975	0.782
8	—	—	—	—	—
9	0.342	0.643	—	0.985	0.985
10	—	—	—	—	—
11	0.282	0.541	0.756	0.909	0.989
12	—	—	—	—	—

$$R_{ph} = R_{slot} \times \frac{Q}{m} \tag{11}$$

Based on the value of current I_{rms} and the resistance of one-phase R_{ph}, the copper losses for m phases are determined as

$$p_{cu} = m \times I_{rms}^2 R_{ph} \tag{12}$$

2.3.3 Mechanical losses: The mechanical losses are produced by friction due to the rotation of the machine. In this study, mechanical losses are neglected.

2.4 Electromagnetic efficiency: The efficiency of the motor is determined by [15]

$$\eta = \frac{P_{out}}{P_{out} + P_{cu} + P_{iron}} \tag{13}$$

where P_{out} is the mechanical power, P_{cu} is the total copper losses of armature and field windings, and P_{iron} is the total iron losses of stator and rotor cores.

3 Summary of analysis solution

The stator windings are fed with a sinusoidal current source and the rotor windings are excited with a DC in order to obtain the target value of torque density. With the limited number of poles ($2_p \leq 10$) for a small machine (3.67 kW/7000 rpm), 15 different machines for different phase/slot/pole combinations are analysed. The excitation current (I_{ext}), the peak value of armature current (I_s), the torque ripple (ΔT), and the machine efficiency (η) are detailed in Table 3.

The torque ripple and the machine efficiency are compared in order to select the most appropriate machine for the application. The torque ripple is a source of noise and vibration, especially in a low-speed machine. Thus, a torque ripple <5% is an important criterion to select the machine for the HVAC application. The seven-phase/seven-slot/six-pole WRSM is selected because it presents the highest efficiency with a torque ripple <5%.

Table 1 Three-, four-, five-, and six-phase windings

$Q\|2_p$	2	4	6	8	10
Three-phase winding					
3	0.866	0.866	—	0.866	0.866
6	—	0.866	—	0.866	0.500
9	0.328	0.617	0.866	0.945	0.945
12	—	—	—	0.866	0.933
15	0.199	0.389	—	0.711	0.866
18	—	0.328	—	0.617	0.735
Four-phase winding					
4	—	—	—	—	—
8	—	—	0.924	—	0.924
12	—	—	—	—	—
16	—	—	0.545	—	0.816
20	—	—	—	—	—
24	—	—	—	—	0.595
Five-phase winding					
5	0.588	0.951	0.951	0.588	—
10	—	0.588	0.809	0.951	—
15	0.205	0.401	0.588	0.732	—
20	—	—	0.448	0.588	—
25	0.123	0.245	0.362	0.474	0.588
30	—	0.205	—	0.401	—
Six-phase winding					
6	—	—	—	—	—
12	—	—	—	—	0.966
18	—	—	—	—	—
24	—	—	—	—	0.605
30	—	—	—	—	—
36	—	—	—	—	0.418

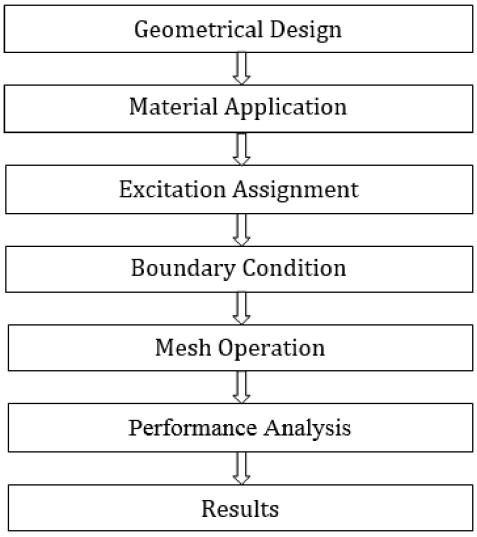

Fig. 1 *Principal steps for modelling*

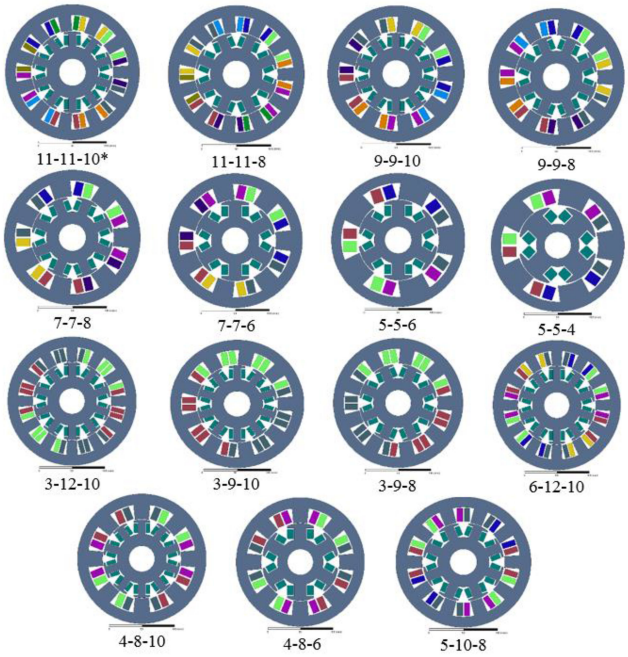

Fig. 2 *WRSM structures (*m–Q–2p)*

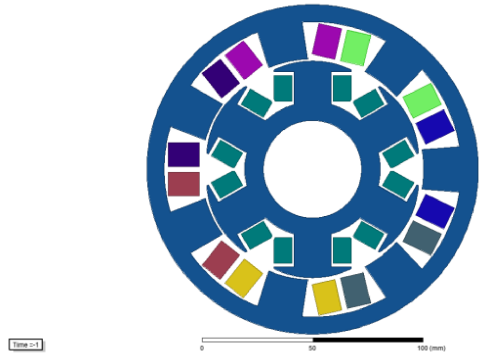

Fig. 3 *Salient-pole WRSM*

4 Comparison with SM-PMSM

A comparison between the chosen WRSM with a reference SM-PMSM has been carried out in order to evaluate the real interest of the structure. A three-phase/nine-slot/eight-pole SM-PMSM with non-overlapping fractional-slot double-layer concentrated winding has been chosen due to its very good performance provided in many studies [16–18]. Both machines are sized on the base of the following criteria:

- Same value of an active volume.
- Same value of torque 5 N m at a rated speed.

The resulting performances of WRSM at rated speed are represented in Table 4.

The performances of SM-PMSM at 7000 rpm using numerical simulations are presented in Table 5.

The performances provided by the WRSM such as torque ripple (3.89%) and efficiency (95%) are close to the SM- PMSM performances.

Furthermore, the comparison of the output power versus speed and the efficiency versus speed between WRSM and SM- PMSM are shown in Figs. 5 and 6. It is important to emphasise that the constant power region of WRSM is wider than SM-PMSM. However, the efficiency at low speed of WRSM is lower than SM-PMSM. This can be explained because for the same active volume the flux generated by rotor winding is smaller than the flux generated by magnet material. To obtain the same value of torque, the stator of WRSM must generate higher flux than that of SM-PMSM, and therefore, the copper losses of WRSM stator are significant.

5 Conclusion

This paper provides the simulation performance of a new brushless WRSM using multiphase non-overlapping fractional-slot double-layer concentrated winding. Several phase/slot/pole models have been selected in order to evaluate the performance using FEM. The simulation results are discussed and demonstrate that the MB-WRSM, which has a high machine performance, has potential to replace PMSM in the HVAC application as it presents a similar performance with a higher fault-tolerance capability.

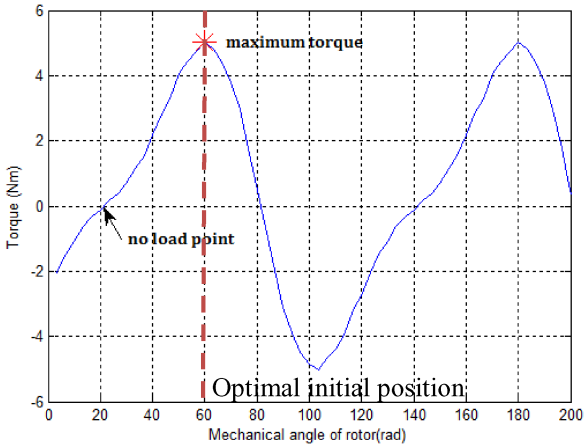

Fig. 4 *Torque versus mechanical rotor angle*

Table 3 Machine performances

$m/Q\|2_p$	I_{ext}, A	I_s, A	ΔT, %	η, %
11/11/10	11.97	4.26	2.46	95.39
11/11/08	13.99	4.42	2.98	95.20
09/09/10	11.14	5.00	3.68	95.16
09/09/08	13.29	5.00	4.78	95.83
07/07/08	12.20	5.85	5.62	95.10
07/07/06	15.58	5.90	4.48	96.15
05/05/06	13.07	7.57	4.32	94.79
05/05/04	19.29	7.57	4.77	95.18
03/12/10	10.29	4.90	13.91	95.03
03/09/10	9.29	5.85	6.57	94.58
03/09/08	11.67	5.80	8.54	95.23
06/12/10	10.00	4.79	9.44	95.22
04/08/10	9.30	6.20	18.19	93.45
04/08/06	13.74	6.40	25.43	95.54
05/10/08	12.80	5.70	81.99	94.88

Table 4 Performance of WRSM

Performance	Value	Unit
field current	3.616	A
armature current	2.912	A
phase voltage	369	V
output power	3.6667	kW
torque ripple	3.89%	—
efficiency	95.03%	—

Table 5 Performance of SM-PMSM

Performance	Value	Unit
armature current	3.5789	A
phase voltage	369	V
output power	3.6667	kW
torque ripple	4.71%	—
efficiency	95.66%	—

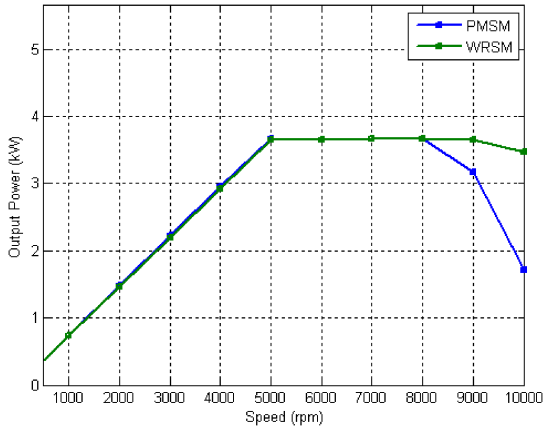

Fig. 5 *Power region of SM-PMSM and WRSM*

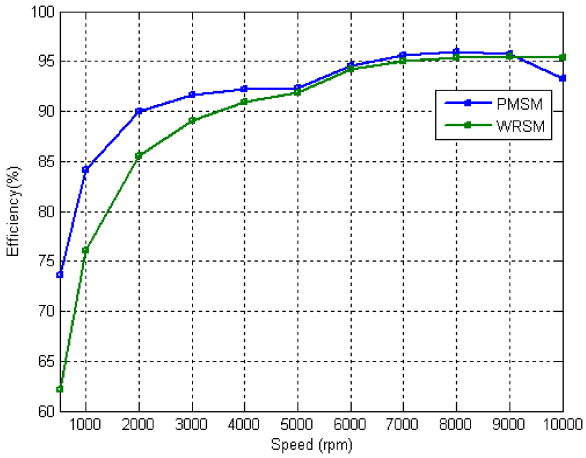

Fig. 6 *Efficiency of SM-PMSM and WRSM*

6 References

[1] Boldea, I., Tutelea, L.N., Parsa, L., *et al.*: 'Automotive electric propulsion systems with reduced or no permanent magnets: an overview', *IEEE Trans. Ind. Electron.*, 2014, **61**, (10), pp. 5696–5710

[2] Widmer, J.D., Martin, R., Kimiabeigi, M.: '*Electric vehicle traction motors without rare earth magnets*' (Elsevier B.V, Duivendrecht, 2015)

[3] Dorrell, D.G.: 'Are wound rotor synchronous motors suitable for use in high efficiency torque dense automotive drives?'. 38th Annual Conf. on IEEE Industrial Electronics Society (IECON), Montreal, Canada, 2012

[4] Ali, Q., Lipo, T.A., Kwon, B.-i.: 'Design and analysis of novel brushless wound rotor synchronous machine', *IEEE Trans. Magnetics*, 2015, **51**, (11)

[5] Jürgens, J., Brune, A., Ponick, B.: 'Electromagnetic design and analysis of a salient pole synchronous machine with tooth-coil windings for use as a wheel hub motor in an electric vehicle'. IEEE, 2014

[6] Gündogdu, T., Kömügöz, G.: 'Implementation of fractional slot concentrated winding technique in large salient-pole synchronous generators'. Power Electronics and Machines in Wind Applications (PEMWA), 2012

[7] Lin, D., Zhou, P., He, B., *et al.*: 'Steady state and transient parameter computation for wound field synchronous machines'. XXth Int. Conf. on Electrical Machines, 2012

[8] EL-Refaie, A.M., Senior Member, IEEE: 'Fractional slot concentrated windings synchronous permanent magnet machines: opportunities and challenges', *IEEE Trans. Ind. Electron.*, 2010, **57**, (1), pp. 107–121

[9] Cros, J., Viarouge, P.: 'Synthesis of high performance PM motors with concentrated windings', *IEEE Trans. Energy Convers.*, 2002, **17**, (2), pp. 248–253

[10] De Donato, G., Capponi, F.G., Rivellini, G.A., *et al.*: 'Integral-slot versus fractional-slot concentrated-winding axial flux permanent magnet machines: comparative design, FEA and experimental tests', *IEEE Trans. Ind. Appl.*, 2012, **48**, (5), pp. 1487–1495

[11] EL-Refaie, A.M., Shah, M.R., Qu, R., *et al.*: 'Effect of number of phases on losses in conduction sleeves of surface PM machine rotors equipped with fractional- slot concentrated windings', *IEEE Trans. Ind. Appl.*, 2008, **44**, (5), pp. 1522–1532

[12] ANSYS Maxwell 2D/3D user's guide

[13] Liu, H., Xu, L., Shangguan, M., *et al.*: 'Finite element analysis of 1 MW high speed wound rotor synchronous machine', *IEEE Trans. Magn.*, 2012, **48**, (11), pp. 4650–4653

[14] Hargreaves, P.A., Mecrow, B.C., Hall, R.: 'Calculation of iron loss in electrical generators using finite-element analysis', *IEEE Trans. Ind. Appl.*, 2012, **48**, (5), pp. 1460–1466

[15] Lee, C.-S., Kim, J.-H., Hong, J.-P.: 'Core loss effects on electrical steel sheet of wound rotor synchronous motor for integrated starter generator', *J. Magnetics*, 2015, **20**, (2), pp. 148–154

[16] Lakshmi Varaha Iyer, K., Minaker, B., Mukherjee, K., *et al.*: 'On-board direct-drive surface permanent magnet synchronous machine with fractional-slot concentrated windings for electric vehicles'. IEEE Canadian Conf. Electrical and Computer Engineering (CCECE), 2016

[17] Junlong, L., Yongxiang, X., Jibin, Z., *et al.*: 'Analysis and design of SPM machines with fractional slot concentrated windings for a given constant power region', *IEEE Trans. Magn.*, 2015, **51**, (11), pp. 34–43

[18] Wang, J., Yuan, X., Atalla, K.: 'Design optimization of a surface-mounted permanent-magnet motor with concentrated windings for electric vehicle applications', *IEEE Trans. Veh. Technol.*, 2013, **62**, (3), pp. 1053–1064